Discriminating between grave sites and non-grave sites using conventional remote sensing methods ©

Julie de Gea, Year 4 of Honours Undergraduate Studies
Supervised by Margaret Kalacska, PhD
Department of Geography, McGill University; Montréal (Québec) Canada

Table of Contents

List of Figures

List of Tables

Abstract

In cases were conventional forensic methods have failed in detecting a clandestine grave and when the search area is extensive, new methods must be applied. The field of remote sensing offers non-invasive methods as to not disturb evidence and can cover an extensive area. It is specifically why remote sensing methods need to be developed for grave site detection, and pertaining to this study, mature grave site detection. Chlorophyll content and vegetation index computed anthocyanin levels have been found to be good indicators for identifying graves versus false graves. Pattern recognition classifiers were proven to not be useful in mature grave detection and should be tested in a controlled environment to establish their true performance. A good chlorophyll content prediction curve can be computed using vegetation indices, particularly RENDVI. Such prediction curves can be applied to airborne imagery so as to classify areas as potential graves. This study is a preliminary study in the detection of mature grave sites using remote sensing methods.

Background

Remote sensing implies acquiring information about a surface without disruption. It is specifically why its application in the forensic domain is being increasingly considered as a way to acquire physical evidence in forensic investigations (Clark Davenport, 2001). Methods with low to no destruction of crime scenes need to be put in place as to not affect evidence that could otherwise be found (Van Belle et al., 2009), explaining the needed use of the remote sensing domain in criminal cases. More closely related to this paper is the detection of mature grave sites where the buried remains have been decomposing for several years. Man-made soil disturbances on the surface are no longer apparent, and low level vegetation such as shrubs and graminoids have taken over. Cases in which the graves have become naturally concealed and in which conventional methods such as eyewitness accounts, informants, or cadaver dogs have failed in locating a murder victim, detection is rendered more difficult. The use of geophysical instruments that have in the past proved their efficacy (ground-penetrating radar, magnetometer, etc.) cannot be implemented, as the location is unknown (Powell, 2004). Concealment naturally lowers the chances of cadaver discovery (Van Belle et al., 2009); in such clandestine situations where body concealment was successful and the search area is extensive, newer methods must be applied.

It had been demonstrated that 'fresh' graves could be identified versus false graves in a tropical environment using the sites' spectral response measured over time (Kalacska et al., 2009). There is however a research gap in the

application of remote sensing methods for grave site detection in a temperate environment, more specifically on older graves.

In the remote sensing domain, objects can be identified based on their reflectance, absorbance, and transmittance properties of light otherwise known as electromagnetic energy. Each surface uniquely reflects parts of the electromagnetic radiation spectrum (Campbell, 2002) or the different wavebands that it comprises according to the object's physical and chemical properties. Sensors can measure such properties outputting a range of recorded reflectance values for each of its channels, also called a spectrum. Current sensors, from spectrometers for ground data to built-in sensors on satellite platforms measure light-to-object interactions from each of its input channels. A channel can measure average reflectance from a larger range of wavebands (multispectral sensor) to a smaller range or even a single waveband (hyperspectral sensor). Acquiring hyperspectral information from a surface should provide a more detailed data set, as each waveband (nm) or nearly each waveband's value can be analyzed. Hyperspectral instruments are more effective than multispectral sensors (Birk and McCord, 1994) based on the quality of the output data set, which can ultimately provide a more effective and accurate discrimination of spectral properties.

Categories of objects or surfaces such as vegetation or roads each have a 'signature' spectrum (Parker and Wolff, 1965). A reflectance graph (mapped reflectance values) of vegetation, regardless of the specie or the geographical location, will always produce a similar shape hence the word 'signature'.

Differences within such category can be noted from intensities of reflectance comparing a range of bands from one leaf to another. Though intra-category or intra-specie differentiation can be difficult, slight differences in chemical composition, moisture content, or surface physical properties can be reflected in the recorded spectral properties. Body decomposition affects the surrounding soil which in turn should affect the spectral response of a grave site (as demonstrated by Kalacska et al., 2009). In turn, the growing vegetation should be affected (depending on the stage of decomposition) and those changes could be mesured from a leaf's spectral response.

Mammalian decomposition occurs in multiple stages starting at the time of death. The decay of organic matter starts with a process called autolysis otherwise known as tissue autodigestion. In this process, liquifaction of the body tissues into basic components (amino acids, etc.) occurs by a chemical breakdown caused by after-death liberated enzymes, bacterial and fungal activity (Campobasso et al., 2001). Autolysis starts at the 'fresh' stage, which then advances to the 'bloating' stage in which the body bloats from the gases produced by internal bacterial activity, decomposition fluids, and from a rapidly growing maggot population if the body is accessible to insect communities. At the start of the 'bloat' stage, a process called putrefaction begins (Lee Goff, 2009), involving the breakdown of proteins by both anaerobic and aerobic bacteria (Campobasso et al., 2001) aided by insect communities. The number of stages in the decomposition process differs in literature (Lee Goff, 2009) but essentially advance to the 'advanced decay' stage and subsequently the 'skeletonization'

stage (involving the dry/remains stages). Early cadaveric materials result in an area of high fertility through 'nutrient pulses' (Stokes et al, 2009), in which the surrounding soil contains high levels of carbon and nutrients such as nitrogen or phosphorus (Carter et al., 2005). The soil pH drastically increases (Benninger et al., 2008) and decomposition gases such as methane can be recorded (Van Belle et al., 2009). The 'advanced decay' stage is characterized with a high nitrogen soil content that has become too toxic to the vegetation on top of a buried decomposing cadaver resulting in a lack of vegetation. All in all however, cadaveric materials from the decomposition process have been linked to an increased biomass production and an increase in species' richness (Towne, 2000).

Many factors affect the rate of decomposition: whether the body is exposed or buried (Vass, 2001), access to the body, soil moisture (Statheropoulos et al., 2007), which also affects the diffusion of nutrients (Carter et al., 2010), and temperature (Lee Goff, 2009). This is why it is often difficult to predict a decomposition stage if the body cannot be clearly observed. In the case of this paper, the bodies have been decomposing for several years and due to the high biomass in the area, the buried bodies have, with certainty, reached the 'remains stage'. Decomposition is a continuous process and the 'remains' stage has no definite end point (Lee Goff, 2009). In this stage, soil concentrations levels of cadaveric nutrients still remain high (Carter et al., 2005): potassium, sodium, or calcium (Vass et al., 1992). The soil also contains elevated concentrations of calcium, phosphorus and manganese from bone breakdown (Carter et al. 2005).

From the high soil nutrient content surrounding body remains, vegetation health differences should be noted based on its growth location near a grave or not.

This study was performed in an old animal graveyard named the 'Parc Safari zoo cemetery,' which contains buried large mammalian cadavers. In this paper, I analyze vegetation spectra from known graves versus known control areas and their average leaf chlorophyll content calculated from ground leaf samples. I analyze applied vegetation indices on collected leaf spectra, and I test the ability of pattern recognition classifiers in separating the grave class vegetation spectra from the control class. The routine was performed over four months to identify seasonality patterns.

From the chlorophyll results and vegetation indices results, I have devise a prediction curve to estimate chlorophyll content from multispectral CASI airborne imagery from the same year and to classify potential grave areas from ground vegetation, specifically chlorophyll mesurements. From the grave and control results in each category of analysis, I have determined whether twelve unknown areas are classifiable as a potential grave or potential non-grave and established the methodology's potential in identifying mature grave sites.

New methods need to be put in place for detecting naturally concealed clandestine graves, particularly in cold cases where the search area is extensive. Establishing differences in ground data from known mature graves and false graves in a particular environment will drastically aid the development of non-intrusive techniques, particularly from airborne imagery, from which the search area could be minimized. Furthermore, it is important to understand seasonality

patterns when surface ground objects are all that we can work with. In this research, I attempt to show the potential of the remote sensing domain in a forensic framework and to establish the possibilities of mature grave site detection in a non-intrusive manner.

Methods

Site Description

The Parc Safari zoo cemetery (Figure 1) is located in Hemmingford, Quebec and has been in operation over the last 50 years. It is located on a local farmer's field that has only been partially disturbed since the last burial. The site contains multiple animal graves for which the times of burial and location have not been documented. Due to a change in cemetery sites in the recent years, it is known that the last burial at the cemetery in question happened some years ago.

The site is located at coordinates 45° 2' 47.5" N and 73° 31' 57.4" W, south of the city of Montreal. The average summer temperature is 19.88°C and the average winter temperature is -5.11°C as per the installed temperature logger on site. The temperatures can go as high as 35°C and as low as -30°C; the area receives a precipitation average of 978.9 cm a year as either snow or rain (National Climate Data and Information Archive, for Montreal Pierre Elliott Trudeau weather station). The climate is considered by the Köppen climate classification as type dfb or as a humid continental climate. The area is located in a conflicting zone between tropical and polar air masses where the temperature differences between seasons are large (Encyclopedia Britannica, Academic

Edition). The cemetery soil is dominantly a Eutric Brunisol of the St. Bernard series derived from a calcerous and dolomitic till (Mailloux and Godbout, 1954). The soil is a shallow well-drained gravelly clay loam with site-recorded soil depths ranging from 25 to 60 cm.

McGill University's anthropology department has been active on the site since 2007 (at the zoo's administration request) for archaeological purposes and education. They have discovered and confirmed the presence, location, and identification of three graves in the cemetery. Even though the three sites have been disturbed to retrieve bones, some of the remains are still present. The surface scars from the excavations remain and have filled up with water since. Two control sites were identified after being searched for remains and none were found. The three graves and the two controls are here used as baseline data to evaluate the ability of the methods described below to discriminate between the two categories. That data was then used to evaluate the categorization potential of unknown areas as a potential grave or non-grave and to evaluate the methodology's potential in detecting mature grave sites.

Sorghum sudanse (Figure 3) leaf samples (an abundant annual invasive specie in the cemetery area) were collected from the three graves (G1, G2, G3), two controls (C1, C2), and twelve areas categorized as 'unknown' numbered from U1 through U12 (locations in Figure 2). The plant's origin in the cemetery is unknown as it is native to the country of Sudan. The true nature of the unknown sites is currently undetermined, as they have not been searched for remains. Since the known grave sites are filled with water, leaf samples were collected

directly around the pits. All ground data was collected on June 4th 2010, August 7th 2010, September 20th 2010, and October 27th 2010 respectively. Data for the month of July is missing due to instrument issues and unavailability. The data from October 2010 only consists of G1, G2, G3, C1, C2, U1, U2, U3, U9, U10, U11, and U12 due do extensive leaf aging at the other sites. For each month, 10 leaf samples were collected per location and analyzed. The samples totaled 170 for each of June, August, and September, and 120 for October for a grand total of 630 samples.

Leaf Spectra Collection/Instrument Description

The leaf samples collected were placed in a cooler right after collection to preserve them until obtaining their individual reflectance spectra in the lab. The time between leaf gathering and obtaining their respective spectra did not exceed 4 hours. The spectra collection was done in the same order as the leaf collection: if G1 leaves were collected first, they were also subject to spectra collection first and so on. After gathering the spectra for each location, the leaves were cut, wrapped in aluminum foil, and placed in the freezer for preservation until they underwent chlorophyll extraction at a later date.

The leaf spectra were collected using an ASD FieldSpec Spectrometer with range 325 nm to 1025 nm (visible to near-infrared of the electromagnetic spectrum). White reference measurements were taken from a 99% reflective Spectralon panel before and between each location's data (every 10 samples). Reflectance for each leaf sample is calculated as a ratio of the raw DN (digital

number) to the Spectralon panel. Dark current measurements were also taken every 50 samples as a means to remove instrument noise.

All spectral information collected before 490 nm and after 900 nm was removed due to extensive noise. The new hyperspectral information cube contained 411 dimensions – or one for each nanometer reading. All leaf spectra were then subjected to the Savitsky-Golay fourth order polynomial smoothing filter in MATLAB to remove any minimally noisy areas. The filter in question is built in the program and was applied with a window size of 31. The vegetation indices and the pattern recognition algorithms' performance described below were calculated using the smoothed spectra.

Chlorophyll Extraction

Each of the collected ground leaves were cut to a standard size of 1 cm by 1 cm and placed in accordingly labeled 15 mL polypropylene centrifuge tubes. Each centrifuge tube was filled with 10 mL of dimethyl sulfoxide (DMSO) to dissolve the chlorophyll pigment from each leaf (Chl*a* and Chl*b*) in order to estimate the total chlorophyll content. From the chlorophyll content, the plants' photosynthetic abilities can be speculated upon, as the higher the chlorophyll content, the better the plant's photosynthetic ability (Curran et al., 1990). The methodology for the chlorophyll extraction follows that of Hiscox and Israelstam (1979). The reason for following this methodology is that the extracted chlorophyll is more stable in a solution of DMSO rather than other proposed solvents: methanol, acetone, methanol, etc. (Richardson et al. 2002).

The centrifuge tubes containing the leaf samples were placed in a preheated water bath at 65°C for a period of 20 minutes and covered to avoid any light interaction. The samples were removed from the water bath and were let to cool. The new solutions were extracted from the centrifuge tubes using plastic disposable pipettes and placed in 5 mL 1 cm path length disposable cuvettes until filled to about 5 mm from the top. The filled disposable cuvettes were placed in a Genesis 10 UV spectrophotometer, calibrated using a cuvette filled with clear DMSO for recording absorbance values. The wavebands for which the values were recorded are 470 nm, 650 nm (Chl*a*), and 666 nm (Chl*b*) respectively. It is important to note that these values are instrument-appropriate and will change from instrument to instrument.

The total chlorophyll content for each leaf for each location was estimated using Arnon's equations in g/L (Arnon, 1949) converted mg per cm^2 according to the leaf sample size placed in the centrifuge tubes. For each month, a dummy variable analysis was applied to calculate the average difference in chlorophyll content from the graves versus the controls. Those results were compared to the chlorophyll content of the unknowns in an attempt to classify the unknowns as a potential grave or non-grave. A one-way analysis of variance was performed for each month and across all months where the all unknowns were put into one single class. This step was performed to make inferences about the variance in each class and to suggest whether the unknown class contains potential graves or not.

Vegetation Indices

A series of commonly used vegetation indices were calculated from the smoothed leaf spectra, particularly those involving plant stress estimations (Figure 4). Only three were retained: PSRI and ARI2 for showing significant differences between grave sites and control sites and RENDVI for chlorophyll content estimation (Gitelson and Merzlyak, 1994).

The PSRI vegetation index estimates levels of senescence from a leaf sample; the PSRI values were originally calculated to compare grave and control values from the later months under analysis and to compare locational differences in the rates of plant aging. Plant senescence is often associated with the degradation of chlorophyll that is gradually being taken over by carotenoids resulting in the yellowing of leaves (Knee, 1972). ARI2 estimates anthocyanin content from leaf samples. Anthocyanin corresponds to a leaf pigment responsible for plant reddening and is particularly abundant in the juvenile and senescing stages of a plant's life; abundant levels of anthocyanin in any stage of plant development is often associated to strong environmental stresses including those induced by soil constituents (Gitelson et al. 2001). In both cases, the higher the resulting value, the greater the plant senescence or the higher the levels of anthocyanins.

Pattern Recognition Classifiers

A number of pattern recognition algorithms were applied to the leaf spectra from the Pattern Recognition Toolbox 4.0 for MATLAB (Duin et al., 2004) also called PRTools. The graves smoothed spectra (G1, G2, G3) were considered as one

class. The grave class was compared to the control class constituting of both C1, and C2 and each of the unknowns. This process was repeated for each of the months to assess classifier performance, and once of all months. For each month under analysis, the grave class contained 30 columns of data (10 for each grave), the control class contained 20 columns of data (10 for each control), and each of the unknowns (U1-U12) contained 10 samples each. For the all-months assessment, the grave class contained 120 samples, the control class 80 samples, and each of the unknowns 30 or 40 samples depending on the October collection. The grave class was compared to the each of the unknowns as opposed to the control class due to the restraining size of the data set. Having a lower number of training samples can affect the forward feature selection process and ultimately classifier performance (Jain and Zongker 1997). The spectra were mixed and divided into 60% training data and 40% testing data. The training data in all cases contained 60% of each data set to be classified (e.g. 60% graves and 60% U1); the same applies to the testing data set, which contained 40% of each class. The data set samples were labeled according to which class they pertained to. The data set was then subjected to PRTools' forward feature selection algorithm, which ranks each band based on percent separability. Using a forward feature selection algorithm optimizes classifier performance, accuracy, result interpretation and reliability (Kudo and Sklansky, 2000, Westen et al., 2001). Furthermore, it allows for feature discovery (Westen et al., 2001) in which consistent bands of high separability could be identified and used to make assumptions on class differences. In each case, the top 25 bands picked by the forward feature selection

algorithm were selected to test each of the classifiers. This was done as a means to standardize the methodology across all months.

The classifiers constituted of two normal density based classifiers: the linear classifier (ldc) and the quadratic (qdc) classifier, and three non-linear classifiers: the Parzen classifier (parzenc) and two neural network classifiers. The first NN classifier (bpxnc) contains three hidden units and is backed by the back-propagation rule (see Heermann and Khazenie, 1992, Paola and Schowengerdt, 1995). The second NN classifier (lmnc) works by the Levenberg-Marquardt rule (see Ranganathan, 2004). The linear and quadratic classifiers both assume normal distribution of the data. The Parzen classifier classifies the data set based on the Parzen density estimation.

The training and testing errors for each classifier was computed; the overall classifier performance was calculated by averaging both the corresponding testing and training errors resulting in a percentage value as overall classification error. Those errors were used to establish classifier performance from separability of the grave and control classes and compared month by month.

Airborne Imagery Classification

Multispectral CASI imagery (Figure 5) was collected on August 7th, 2010 at 12:30 PM local time over the Parc Safari cemetery site with a sensor elevation of 1000 m. The flight lines were merged and geo-corrected and the standard deviation of the bands was estimated prior to acquisition. The CASI image contained 10 bands ranging from 488.88 nm to 900.73 nm with a pixel size of 0.8

m by 0.8 m. Atmospheric correction was performed on the imagery (converted to a BIL file format) in ENVI 4.7 using FLAASH with the corresponding flight parameters and a ground elevation of 264 feet. Vicarious calibration was performed next in MATLAB, outputting a gains file by dividing the ground asphalt spectrum and the corresponding imagery ROI mean asphalt spectrum (scaled to ground reflectance). The gains file (which corrects the airborne imagery according to ground spectra) was applied to the imagery as a final calibration process.

A chlorophyll prediction curve was computed in TableCurve 2D v5.01 using all chlorophyll results for all months against the corresponding log base 2 RENDVI values calculated from the smoothed spectra. RENDVI values from the imagery were calculated in ENVI using bandmath following the equation in Figure 4. The corresponding log base 2 values were computed in the same manner. The output prediction curve with the best adjusted R^2 result was applied to the imagery to estimate vegetation chlorophyll content. Potential grave sites were classified using the density slice option in ENVI, for which the classes were derived from ground chlorophyll data from the month of August. Because the imagery calculated chlorophyll was scaled by a factor of 2, the ground data results were scaled accordingly. All values below the dummy variable cut-off for the grave chlorophyll content were classified as a potential non-grave. All values above were classified as a potential grave. Other areas: road, water, etc. were put in a separate class.

Results/Discussion

Significant differences can be found in the spectra from the graves versus the controls as shown in Figure 6. The reflectance spectra of the graves show differences, particularly in the near-infrared region, for the months of June and September. A likely explanation for the average grave spectrum's increased reflection in the NIR for those months is a difference in the internal cellular structure of the plant; levels of hydration in the cellulose walls (Knipling, 1970) is a possibility. The average spectra for each of the grave and control class in the month of August overlaps and presents no difference anywhere on the reflectance graph. Because of spectral differences in the reflectance in other months, seasonality patterns in *Sorghum sudanse* near graves and controls should be noted.

The chlorophyll extraction results can be found in Figure 7, which shows the sample mean for each location for each month in mg per cm^2. The highest chlorophyll content values occur in the month of June with the graves having significantly higher chlorophyll contents that all other locations. The results show stabilization of the of the grave's chlorophyll content in the month of August where the chlorophyll content of the grave leaves have decreased and the chlorophyll content of all other locations have increased, resulting in similar results across all classes. The August chlorophyll content results coincide with the spectral averages in Figure 6, where no notable differences in reflectance can be observed in the average spectra of the two classes. Chlorophyll content differences can again be noted in the months of September and October where the

graves show higher chlorophyll values than the controls, the values of which have decreased. The U6 location content peaks up in the months of August and September with values close to the grave values. Table 1 shows the dummy analysis test on all chlorophyll data for each month. The control value represents how much chlorophyll should be found in a control, and the grave value represents how much more chlorophyll can be found in a grave relative to a control leaf sample. The dummy test failed for the month of August supported by the average values in Figure 7 in which the chlorophyll content for the graves and controls are very similar. Using the grave threshold from the dummy analysis for all statistically significant results (June, September, and October), the unknowns could be potentially classified. None of the unknowns can be classified as a potential grave for the month of June. For the month of September, U1, U2, U3, U6, U8, U9, U10, U11, and U12 could all be classified as potential graves. In the month of October, from the available data, U1, U2, U9, U10, U11, and U12 could be classified as potential graves. However, C1 falls in the threshold for the month of September, strongly implying the chances of false positives. Furthermore, none of the unknowns can be classified in either June or August, which brings us to the conclusion that classifying the unknowns from the chlorophyll results of the graves using this particular data set is doubtful. Another important point to note is that soil moisture increases the diffusion of soil nutrients (Carter et al., 2010). All grave leaves were collected around the grave water pits, and though soil moisture was not measured, it is fair to assume that higher soil moisture for the graves could potentially have an effect on the

chlorophyll values. Furthermore, it is a problem to not know the age of the graves, as they could be far more recent than any potential graves near the unknowns. Because all unknown locations are fairly scattered through the graveyard, the potential for at least one unknown to be near a grave is high, suggesting that chlorophyll data from known graves with different ages could aid in classifying the unknowns.

Figure 8 shows the chlorophyll content across all months for visualization purposes. Due to changes across the months during which the data was collected, the chlorophyll data from all months combined should not be used to derive conclusions. However, even combining all chlorophyll data from all months under analysis shows a relatively strong difference in the leaf chlorophyll content between the graves and controls. In the same figure, U6 with its combined values shows similar chlorophyll content results as the graves with very close means. Figure 9 shows a graphed one-way analysis of variance for each month, and all months combined. In this case, the unknowns were put into one class to analyze the variance across all the unknowns. The month of August shows similar results across all classes as expected from the mean contents in Figure 7. For all other months and all months combined, large variances in the grave class are observed possibly due to the environment from which the leaves were collected. Furthermore, G1 leaves were collected around a deeper pit than G2 and G3, which may affect access to nutrients. G1 chlorophyll content means from Figure 7 are generally lower than G2 and G3, explaining the large variances in Figure 9. In terms of the unknown class, the results meet the controls and graves in the

middle. Variance for each graph is relatively strong, suggesting that some of the unknowns are potential graves. However, classifying the unknowns from the monthly chlorophyll data in this case is doubtful. The U6 location may also be affecting the unknown class ANOVA graphs as the chlorophyll content in two of the three months was significantly higher that other unknowns.

In the case of this research, it would be vital to have more known grave sites and control sites with known grave ages. Knowing the grave ages could provide inferences on the changing patterns of chlorophyll content from a relatively recent grave to a more mature grave. For further research, all locations should be in a similar plant growth environment where soil moisture is controlled. Such data set could provide more reliable results for chlorophyll content assumptions and for deriving chlorophyll seasonal patterns. All in all, a greater chlorophyll content can be observed from the grave sites as opposed to the controls. As we go further in the data set, there is stronger evidence that at one point in *Sorghum sudanse* plant phenology, graves and false graves cannot be distinguished either in the spectra of in the chlorophyll content,possibly due to environmental factors (see all data for August 7th, 2010).

As previously noted, none of the plant indices calculated showed significant differences between the graves and controls but for PSRI (plant senescence) and ARI2 (anthocyanin content). Those results can be found in Figure 10, which shows changes in the calculated values from month to month. Seasonal patterns can once more be observed to be coinciding with the spectra and chlorophyll results for the month of August. The length of each of the coloured bars on the

scale represents the PSRI or ARI2 value for that particular month and particular location. The differences in values across all locations can be noted from the size difference of each bar. In cases where the October bar is not present, the data is absent (no leaf sample collection for certain locations in October due to extensive plant aging). The PSRI values for the graves are much higher than the controls for the months of June, September and October. The values for August across the two classes are similar. The fact that the PSRI values for the graves are higher than the controls does not make sense according to the chlorophyll results, particularly for the months of September and October where plant senescence should be examined. For both months, chlorophyll content values are higher for the graves than the controls, which coincides with a lower rate of plant aging. Plant senescence is often related to degradation of the chlorophylls (Merzlyak et al.,1999) and a degradation in the carotenoids (Biswall, 1995). No significant results were found from either of the CRI1 and CRI2 vegetation indices. Furthermore, differences in plant senescence are observed in the month of June, when plants were not, and should not, be senescing unless it were to be caused by environmental factors. In the month of September, PSRI values for some locations (particularly the graves) increased drastically, only to drop in October. This questions the legitimacy of the equation used and the wavebands it involves. Nonetheless, the equation for plant senescence shows important differences between the graves and the controls. In the case of PSRI, U6 again shows similar results to the graves.

ARI2 results show consistently higher values for the graves than the controls, except for the month of August for which the values are similar. Because the vegetation indices were computed from the spectra, the VI results should follow a similar trend. U6 again shows similar results to the graves except for the month of June, which coincides with the chlorophyll extraction data. The levels of leaf anthocyanins are often associated with environmental stresses; since the values differ from location to location, soil constituents (Gitelson et al. 2001) are probably the main cause for higher levels of anthocyanins in the grave leaves. G1 results follow the same trend as its corresponding chlorophyll results. Thus far, the results from all methodologies coincide with one another. Anthocyanin levels can be used as a good indicator of differentiation between graves and false graves, as is the chlorophyll content. Again, classification of the unknowns is difficult as it is from the chlorophyll data. As mentioned, analyzing graves of known ages and with a similar environment to the unknowns would help in potential classification.

The pattern recognition classifier results can be found in Tables 2 through 6. The values in the tables represent the overall classification error for each classifier. Each of the locations was compared to the grave class resulting in two classes per run. The value for a location under a specific month is the classification error (for the classifier that it represents) in separating the grave class from the location spectra. In an ideal situation, the grave class and the control class should have minimal error. Each of the normal densities linear classifier (Table 2), the neural network by backpropagation rule classifier (Table

3), and the Parzen classifier (Table 4) show strong inconsistencies across all months for each location. In some instances, the graves and controls could not be separated when in other instances it could. Those classifiers do not follow the trends from previous analyses. The quadratic classifier shows poor results (high overall classification error) for all comparisons across all months. However, comparing the data from all months combined, that quadratic classifier's performance is considered very good with an ability to separate the control class from the grave class with an overall error of 19%. In a real life data set, such result is promising. However, for all the locations for which the October data is missing, the quadratic classifier does not perform well with high overall errors. This coincides with a lower number of training and testing samples. It has been noted in literature that a small sample size can affect classifier performance from inferior results by the forward feature selection (Jain and Zongker, 1997). Estimation problems can also occur with a small data set as variances in parameter estimates can cause deviations between the training and testing data (Kraaijveld, 1996) resulting in a high overall classification error. The use of the quadratic classifier in this case, should be limited to large data sets and cannot be used to classify the unknowns as a potential grave or non-grave. The neural network by the Levenberg-Marquardt rule is probably the most reliable classifier in terms of class separation. Though some inconsistencies exist across the months, out of all the classifiers analyzed, it shows the best results with either separation or non-separation for each location. However, based on poor separation for the control class versus the grave class in the months of August

and September, confidently classifying the unknowns as a potential grave or potential non-grave is not possible. In this case, the methodology has failed in not only separating the control class from the grave class but also in potentially classifying the unknowns. Based on those results, pattern recognition classifiers should not be used in the identification of mature graves. Another important to note is that soil constituents may change based on grave age. Such can show differences in some waveband values and ultimately affecting classifier performance. Classifiers may then be able to separate a grave from another grave by using the forward feature selection algorithm in selecting the top bands of separation. Classifiers in the case of this study should not be used. It would however be interesting to test classifiers over graves of different ages and in controlled environments.

The forward feature selection results, from which the classifiers were evaluated, can be found in Figure 11. This further shows the inability of the forward feature selection algorithm to rate similar ranges of bands accordingly across all months. No bands could be identified that repeatedly came up at the top of the forward feature selection results. It is likely in this case, that the forward feature selection algorithm significantly affected classifier performance. Since strong variations in the chlorophyll content of the graves can be observed, it is likely that there are also strong variations in the grave spectra, affecting the forward feature selection process and classifier performance from training to testing data.

The prediction curve obtained from the TableCurve 2D analysis is graphed in Figure 12. The prediction curve for chlorophyll as a function of log base 2 RENDVI values with an adjusted R^2 of 0.51 is as follow:

Chl (mg/cm²) = -0.030841137 + (-0.099339052 / log RENDVI)

It has been demonstrated in literature that RENDVI is a good vegetation index for the estimation of chlorophyll (Gitelson and Merzlyak, 1994). The density slice classified map from the CASI imagery can be found in Figure 13. The threshold for the classification was obtained from the August dummy test for chlorophyll ground data multiplied by 2 as the chlorophyll results from the imagery were scaled as such. Because the dummy test for the August data was not statistically significant, the mapped classification from the imagery should not be considered statistically significant either. In fact, the graves do not come up in the classification as 'potential graves' when the controls area (which was found to contain no bodies) is classified as a potential grave site. This is mostly due to chlorophyll values being similar across all classes in August; in such a case, applying a threshold will only give false positive or false negatives. Because the imagery was taken in the month of August, the August dummy test for chlorophyll had to be used. In the case of this study, soil data was not collected and such should be considered when classifying imagery as it was performed. For future research, acquiring airborne hyperspectral imagery would also provide more accurate results. In the case of the CASI imagery, the closest bands to the RENDVI equation were used rather than exact mentioned band, which ultimately skews the results from the prediction curve. Imagery over the site under analysis

should be taken every day of ground data collection in order to conclude if imagery-based classification coincides with ground data. If a large enough data set is built, grave search over airborne imagery is a strong possibility.

Conclusion

Significant differences in the chlorophyll content indicate that chlorophyll could be used as an indicator of a buried decomposing body at a later stage in the decomposition process. The same goes for leaf anthocyanin content for which grave leaves appear to contain at a significantly higher level. Seasonality patterns are observed across the months for both the chlorophyll content and VI calculated anthocyanin content; patterns that should be noted in future research. Classification of the unknowns is doubtful using all data sets, as the grave values are generally too high to make inferences. It is possible that the growing environment of grave leaves near water pits has an effect on the recorded and calculated values of chlorophyll and anthocyanins, which rendered classification of the unknowns possibly inconclusive. Pattern recognition classifiers over vegetation spectra failed in not only separating between controls and graves in some instances, but also in classifying the unknowns; their use should be tested in a controlled environment. A good prediction curve can be computed by estimating chlorophyll using the log of RENDVI values and classification of imagery from ground data, which is possible if the ground data differences are statistically significant. For further research, more vegetation data should be acquired over a larger number of controls and graves. Testing chlorophyll and anthocyanin levels

over graves of different ages could be significant in establishing a pattern across ages which would distinctly help in forensic investigations. All collection sites should be located in a similar growth environment to avoid large variances errors in the results. Hyperspectral airborne imagery should be collected during each day of data collection to test the accuracy of airborne classification from ground data. The detection of mature grave sites using remote sensing methods is possible and needs to be developed further across a wide range of studies to standardize methodologies and provide a complete data set which would be useful for forensic investigations.

References

Arnfield, A. J. Koppen climate classification (climatology) -- Britannica Online Encyclopedia. *Encyclopedia - Britannica Online Encyclopedia*. Available at: http://www.britannica.com/EBchecked/topic/322068/Koppen-climate-classification

Arnon, D. I. (1949). Copper Enzymes in isolated chloroplasts. Polyphenoloxidase in *Beta vulgaris*. *Plant Physiology*, *24*, 9-15.

Benninger, L. A., Carter, D. O., & Forbes, S. L. (2008). The biochemical alteration of soil beneath a decomposing carcass. *Forensic Science International*, *180*, 70-75.

Birk, R. J., & McCord, T. B. (1994). Airborne Hyperspectral Sensor Systems. *IEEE AES Systems Magazine*, *1*, 26-33.

Biswal, B. (1995). Carotenoid catabolism during leaf senescence and its control by light. *Journal of Photochemistry and Photobiology B: Biology*, *30*, 3-13.

Campbell, J. B. (2002). Foundations. *Introduction to Remote Sensing* (pp. 3-26). New York: The Guilford Press.

Campobasso, C. P., Vella, G. D., & Introna, F. (2001). Factors affecting decomposition and Diptera colonization. *Forensic Science International*, *120*, 18-27.

Canadian Climate Normals 1971-2000. *Canada's National Climate Archive*. Available at: http://climate.weatheroffice.gc.ca/

Carter, D. O., Yellowlees, D., & Tibbett, M. (2007). Cadaver decomposition in terrestrial ecosystems. *Naturwissenschaften*, *94*, 12-24.

Carter, D. O., Yellowlees, D., & Tibbett, M. (2010). Moisture can be the dominant environmental parameter governing cadaver decomposition in soil. *Forensic Science International*, *200*, 60-66.

Davenport, G. C. (2001). Remote Sensing Applications in Forensic Investigations. *Historical Archaeology*, *35*(1), 87 - 100.

Duin, R. P. W., Juszczak, P., de Ridder, D, Paclík, P., Pekalska, E., & Tax, D. M. J. (2004). PR-Tools 4.0 : a Matlab Toolbox for Pattern Recognition. http://www.prtools.org

Curran, P. J., Dungan, J. L., & Gholz, H. L. (1990). Exploring the relationship

between reflectance red edge and chlorophyll content in slash pine. *Tree Physiology*, *7*, 33-48.

Gamon, J. A., Lee, L. F., Qiu, H. L., Davis, S., Roberts, D. A., & Ustin, S. L. (1998). A multi-scale sampling strategy for detecting physiologically significant signals in AVIRIS imagery *in Seventh Annual JPL Airborne Earth Science Workshop*, *January 12-16, NASA JPL*, California, 1998.

Gitelson, A., & Merzlyak, M. N. (1994). Quantitative estimation of chlorophyll-a using reflectance spectra: experiments with autumn chestnut and maple leaves. *Journal of Photochemistry and Photobiology B: Biology*, *22*, 247-252.

Gitelson, A. A., Merzlyak, M. N., & Chivkunova, O. B. (2001). Optical properties and non-destructive estimation of anthocyanin content in plant leaves. *Photochemistry and Photobiology*, *74*, 38-45.

Gitelson, A. A., Zur, Y., Chivkunova, O. B., & Merzlyak, M. N. (2002). Assessing carotenoid content in plant leaves with reflectance spectroscopy. *Photochemistry and Photobiology*, *75*, 272-281.

Hiscox, J. D., & Israelstam, G. F. (1979). A method for the extraction of chlorophyll from leaf tissue without maceration. *Canadian Journal of Botany*, *57*, 1332-1334.

Humid Continental Climate. *Britannica Online Encyclopedia*. Available at: http://www.britannica.com/

Jain, A., & Zongker, D. (1997). Feature Selection: Evaluation, Application, and Small Sample Performance. *IEEE Transactions on Pattern Analysis and Machine Intelligence*, *19*, 153-158.

Kalacska, M. E., Bell, L. S., Sanchez-Azofeifa, G. A., & Caelli, T. (2009). The Application of Remote Sensing for Detecting Mass Graves: and Experimental Animal Case Study from Costa Rica. *Journal of Forensic Sciences*, *54*, 159 - 166.

Knee, M. (1972). Anthocyanin, carotenoid, and chlorophyll changes in the peel of Cox's orange pippin apples during ripening on and off the tree. *Journal of Experimental Botany*, *23*, 184-196.

Knipling, E. B. (1970). Physical and Physiological Basis for the Reflectance of Visible and Near-Infrared Radiation from Vegetation. *Remote Sensing of Environment*, *1*, 155-159.

Kraaijveld, M. A. (1996). A Parzen classifier with an improved robustness

against deviations between training and test data. *Pattern Recognition Letters*, *17*, 679-689.

Kudo, M., & Sklansky, J. (2000). Comparison of algorithms that select features for pattern classifers. *Pattern Recognition*, *33*, 25-41.

Goff, M. L. (2009). Early post-mortem changes and stages of decomposition in exposed cadavers. *Experimental and Applied Acarology*, *49*, 21-36.

Heermann, P. D., & Khazenie, N. (1992). Classification of Multispectral Remote Sensing Data Using a Back-Propagation Neural Network. *IEEE Transactions on Geoscience and Remote Sensing, 30*, 81-88.

Mailloux, A., & Godbout, G. (1954). Etude Pédologique du Comté de Huntingdon et Beauharnois. *Province de Quebec - Ministere de l'Agriculture*, *1*, 1-184.

Merton, R. N. (1998). Multi-temporal analysis of community scale vegetation stress with imaging spectroscopy. University of Auckland, Auckland, NZ, 1998.

Merzlyak, M. N., Gitelson, A. A., Chivkunova, O. B., & Rakitin, V. Y. (1999). Non-destructive optical detection of pigment changes during leaf senescence and fruit ripening. *Physiologia Plantarum*, *106*, 135-141.

Paola, J. D., & Schowengerd, R. A. (1995). A Detailed Comparison of Backpropagation Neural Network and Maximum-Likelihood Classifiers for Urban Land Use Classification. *IEEE Transactions on Geoscience and Remote Sensing*, *33*, 981-996.

Parker, D. C., & Wolff, M. F. (1965). Remote Sensing. *International Science and Technology*, *43*, 20-31.

Powell, K. (2004). Detecting buried human remains using near-surface geophysical instruments. *Exploration Geophysics*, *35*, 88-92.

Ranganathan, A. (2004). The Levenberg-Marquardt Algorithm. *Georgia Tech College of Computing*, *1*, 1-5.

Richardson, A. D., Duigan, S. P., & Berlyn, G. P. (2002). An evaluation of noninvasive methods to estimate foliar chlorophyll content. *New Phytologist*, *153*, 185-194.

Rouse, J. W., Haas, R. H., Schell, J. A., & Deering, D. W. (1973). Monitoring vegetation systems in the Great Plains with ERTS *in NASA: Goddard Space Flight Center 3rd ERTS-1 Symposium*, *1*, 309-317.

Statheropoulos, M., Agapiou, A., Spiliopoulou, C., Pallis, G. C., & Sianos, E. (2007). Environmental aspects of VOCs evolved in the early stages of human decomposition. *Science of The Total Environment*, *385*, 221-227.

Stokes, K. L., Forbes, S. L., Benninger, L. A., Carter, D. O., & Tibbett, M. (2009). Decomposition Studies Using Animal Models in Contrasting Environments: Evidence from Temporal Changes in Soil Chemistry and Microbial Activity. *Criminal and Environmental Soil Forensics* (pp. 357-377). International: Springer Science and Business Media.

Towne, E. G. (2000). Prairie vegetation and soil nutrient responses to ungulate carcasses. *Oecologica*, *122*, 232-239.

Van Belle, L. E., Carter, D. O., & Forbes, S. L. (2009). Measurement of ninhydrin reactive nitrogen influx into gravesoil during aboveground and belowground carcass (Sus domesticus) decomposition. *Forensic Science International*, *193*, 37-41.

Vass, A. A., Bass, W. M., Wolt, J. D., Foss, J. E., & Ammons, J. T. (1992). Time since death determinations of human cadavers using soil solution. *Journal of Forensic Science*, *37*, 1236-1253.

Vass, A. A. (2001, November). Beyond the grave - understanding human decomposition. *Microbiology Today*, *28*, 190-192.

Weston, J., Mukherjee, S., Chapelle, O., Pontil, M., Poggio, T., & Vapnik, V. (2001). Feature selection for SVMs. *Advances in Neural Information Processing Systems*, *13*, 668 - 674.

Appendix.

Figure 1 : Parc Safari Zoo cemetery view

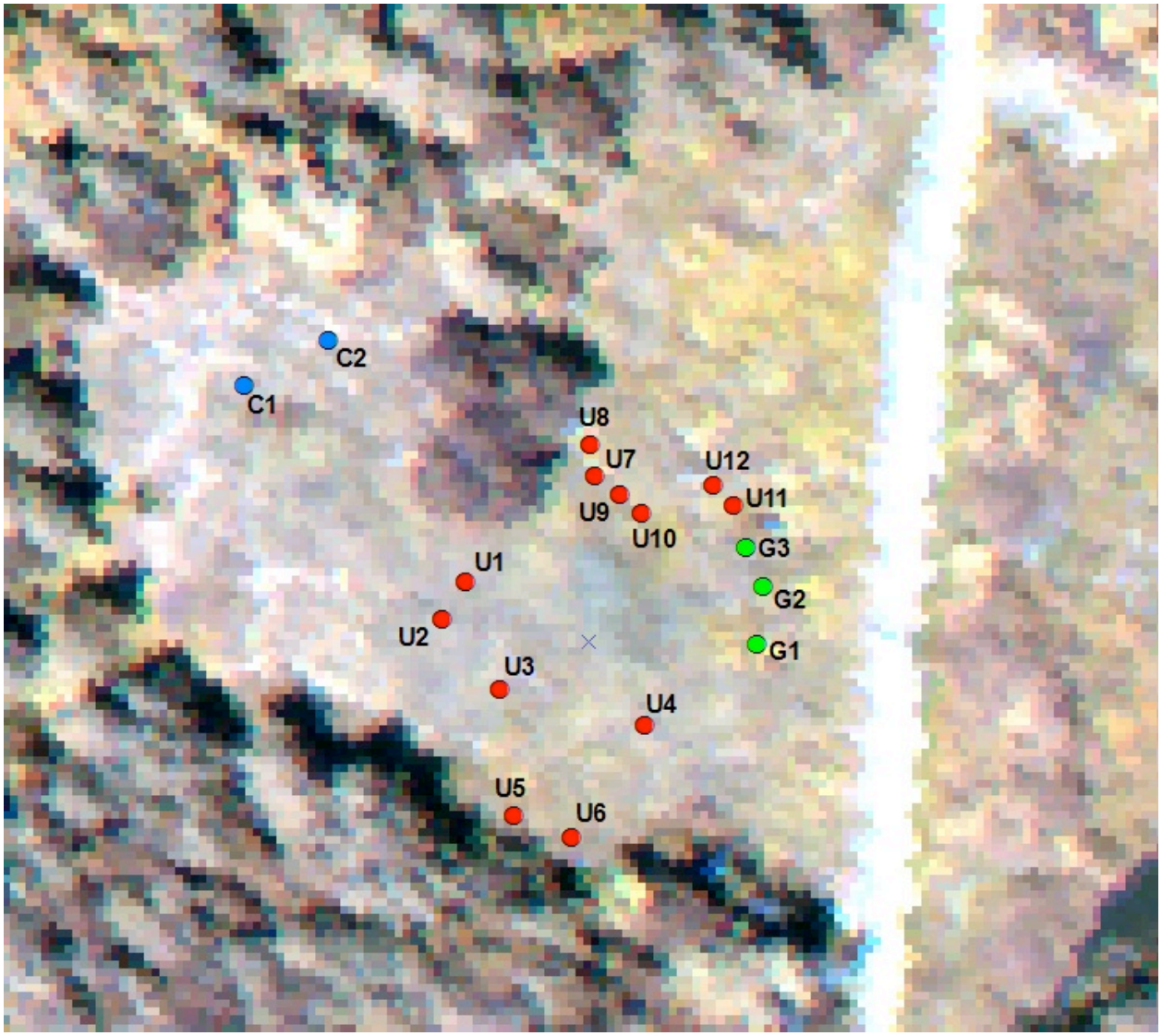

Figure 2 : Map locations for all data collection points

Figure 3 : *Sorghum sudanse* sample

Vegetation Index	Description	Equation	Reference
$NDVI$	Normalized Difference Vegetation Index	$\frac{b750-b680}{b750+b680}$	Rouse et al (1973)
$RENDVI$	Red-edge Normalized Difference Vegetation Index	$\frac{b750-b705}{b750+b705}$	Gitelson & Merzlyak (1994)
PRI	Photochemical Reflectance Index	$\frac{b531-b570}{b531+b570}$	Gamon et al (1998)
$PSRI$	Plant Senescence Reflectance Index	$\frac{b680-b500}{b750}$	Merzlyak et al (1999)
$RVSI$	Red-edge Vegetation Stress Index	$\frac{b714+b752}{2} - b733$	Merton (1998)
$CRI1$	Carotenoid Reflectance Index 1	$\frac{1}{b510} - \frac{1}{b550}$	Gitelson et al (2002)
$CRI2$	Carotenoid Reflectance Index 2	$\frac{1}{b510} - \frac{1}{b700}$	Gitelson et al (2002)
$ARI2$	Anthocyanin Reflectance Index 2	$b800\left(\frac{1}{b550} - \frac{1}{b700}\right)$	Gitelson (2001)

Figure 4 : List of vegetation indices applied on collected leaf spectra

Figure 5 : CASI imagery from August 2010

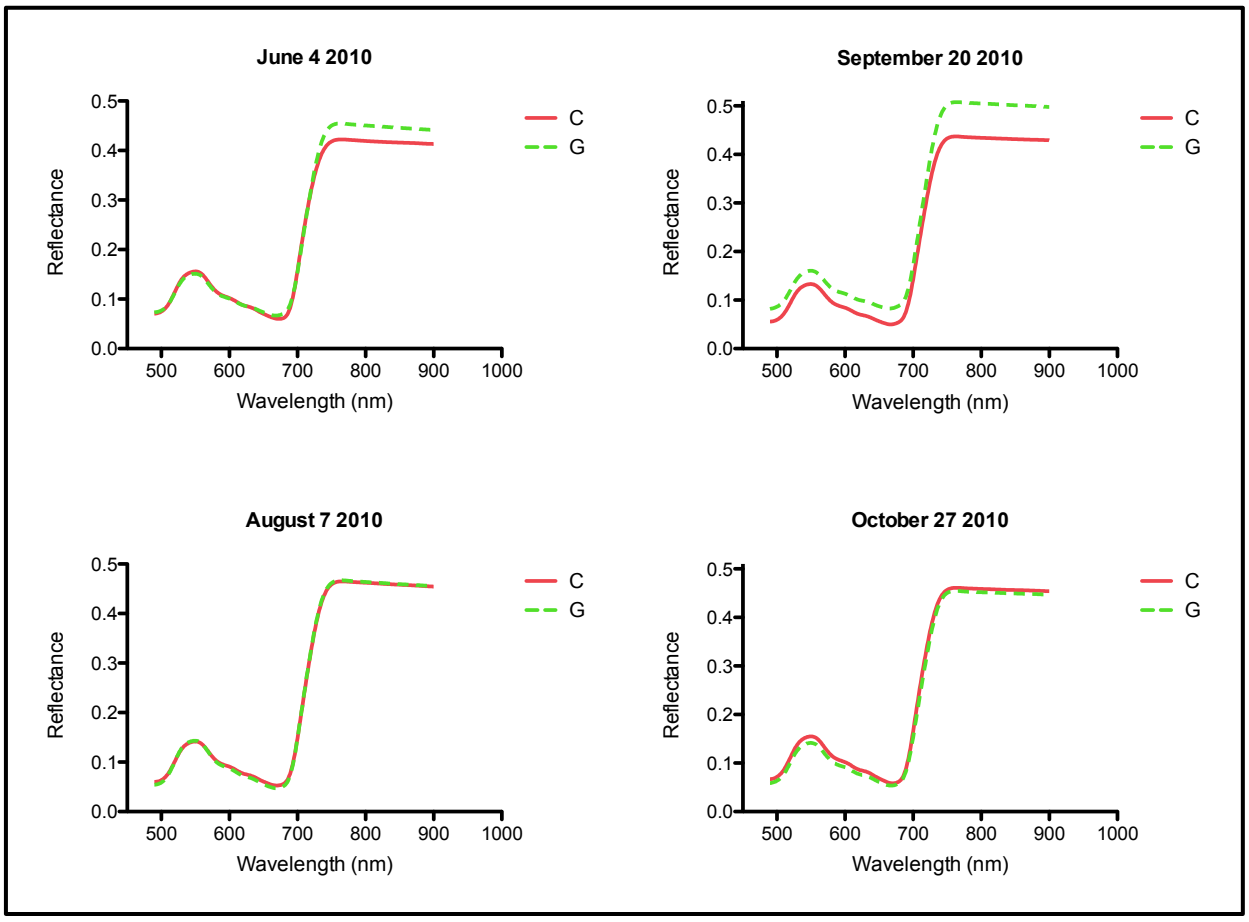

Figure 6 : Average leaf spectra for the grave and control classes

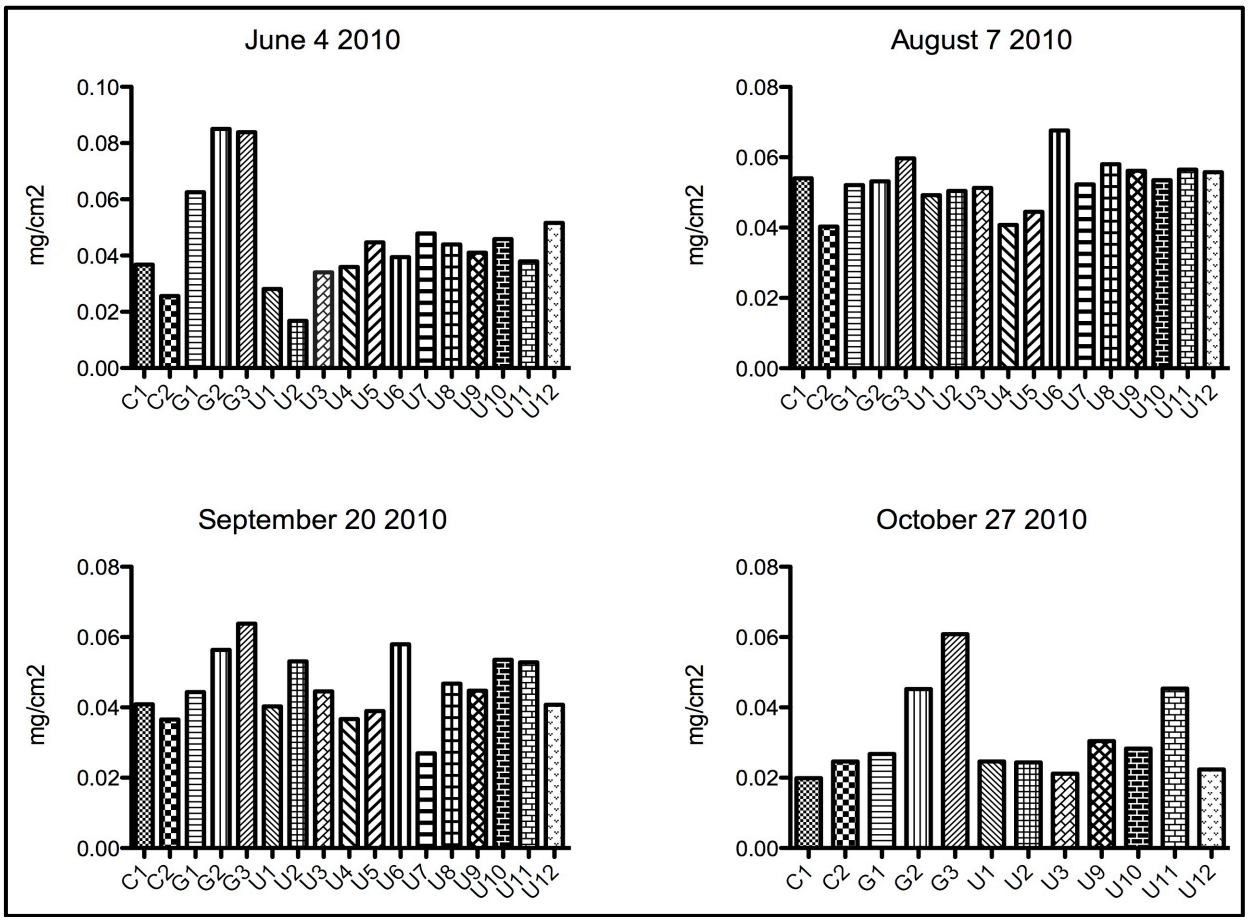

Figure 7 : Chlorophyll extraction content means for each collection date

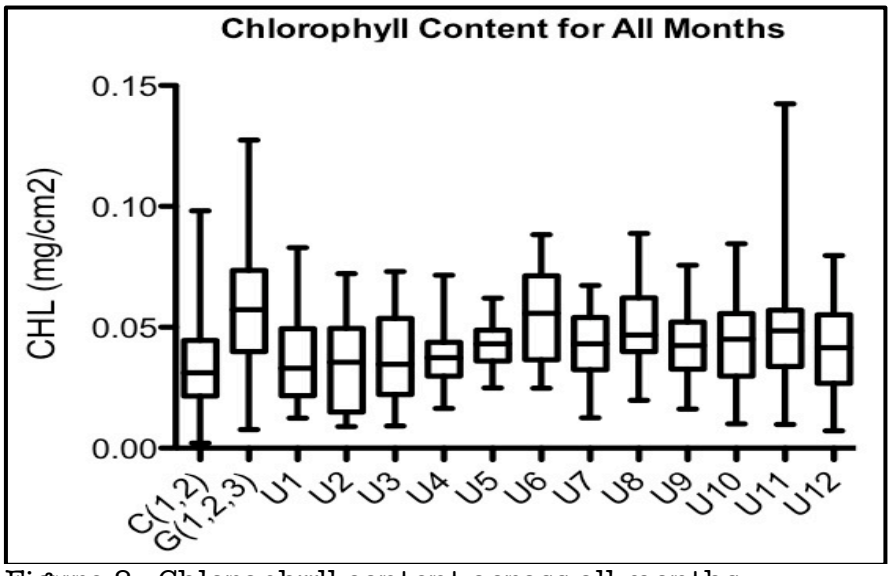

Figure 8 : Chlorophyll content across all months

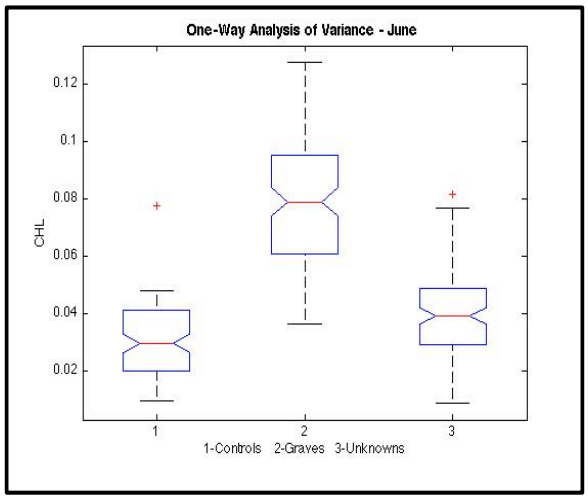

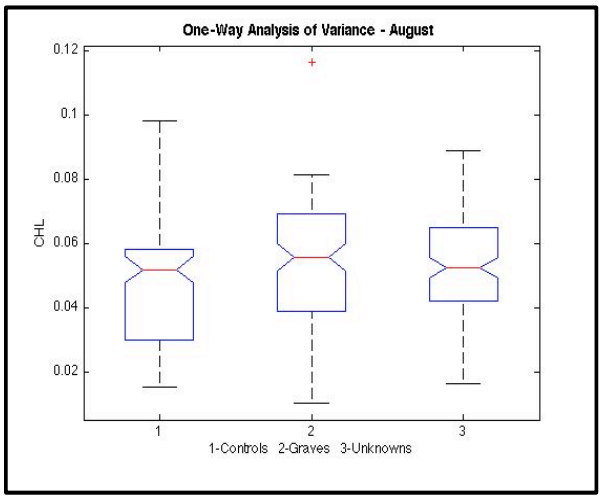

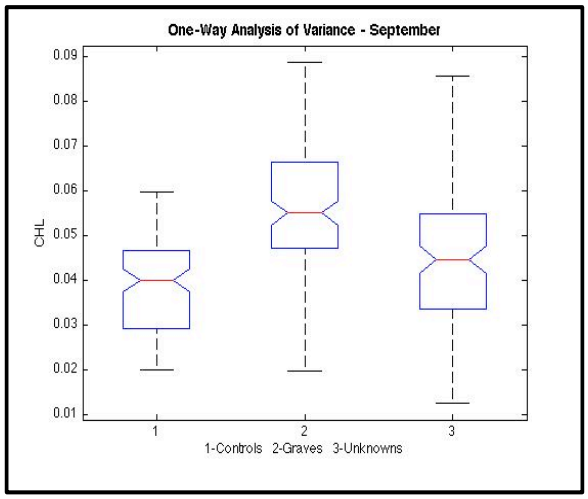

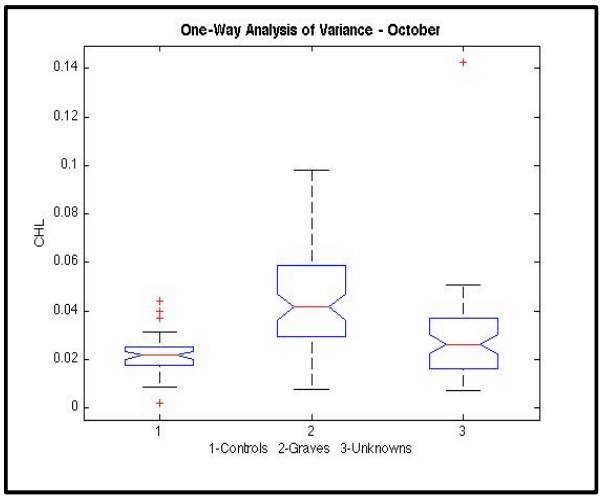

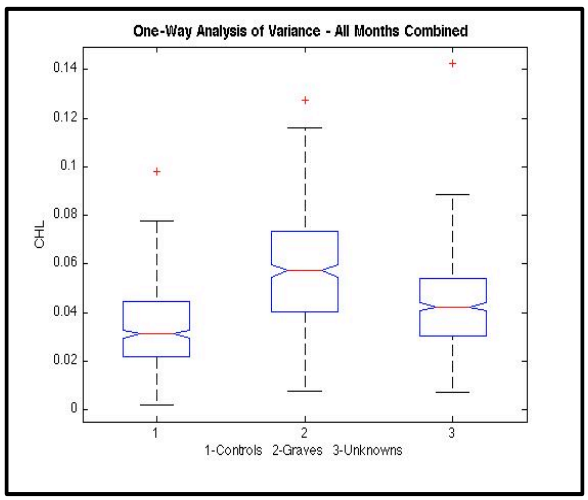

Figure 9 : ANOVA results for the grave, control, and unknown classes for each month and all months combined

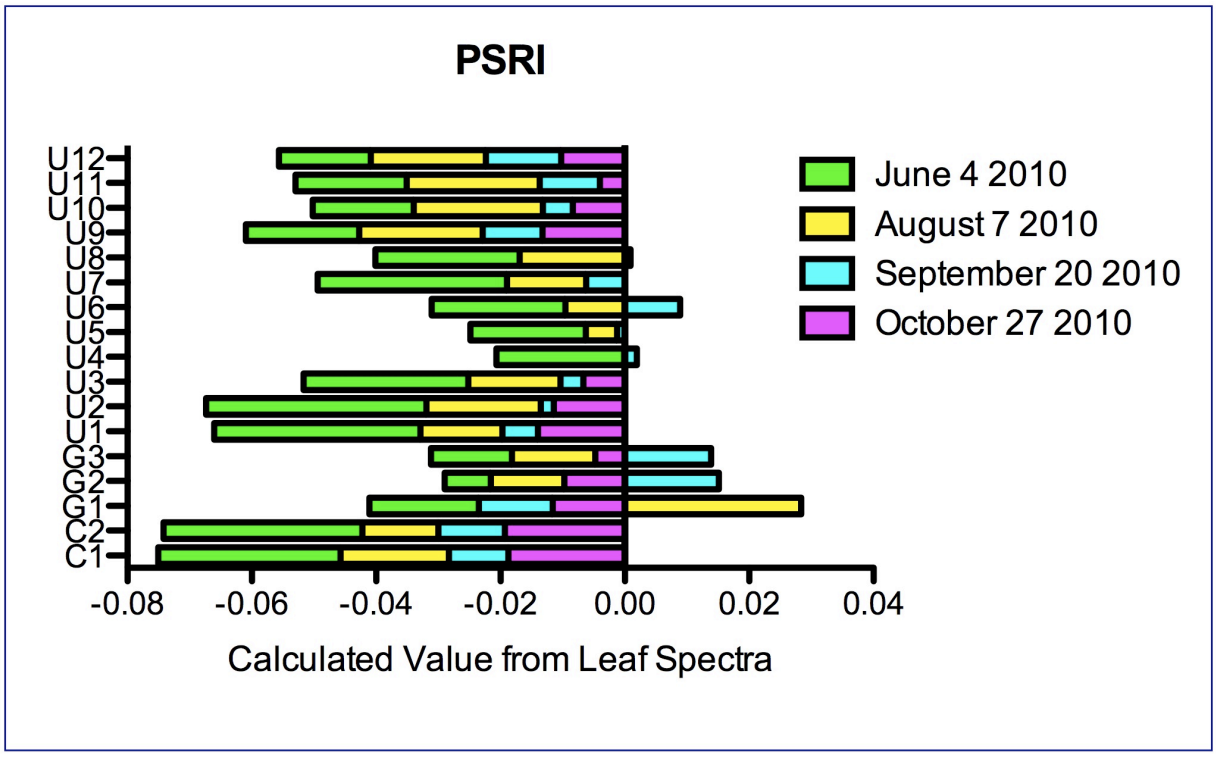

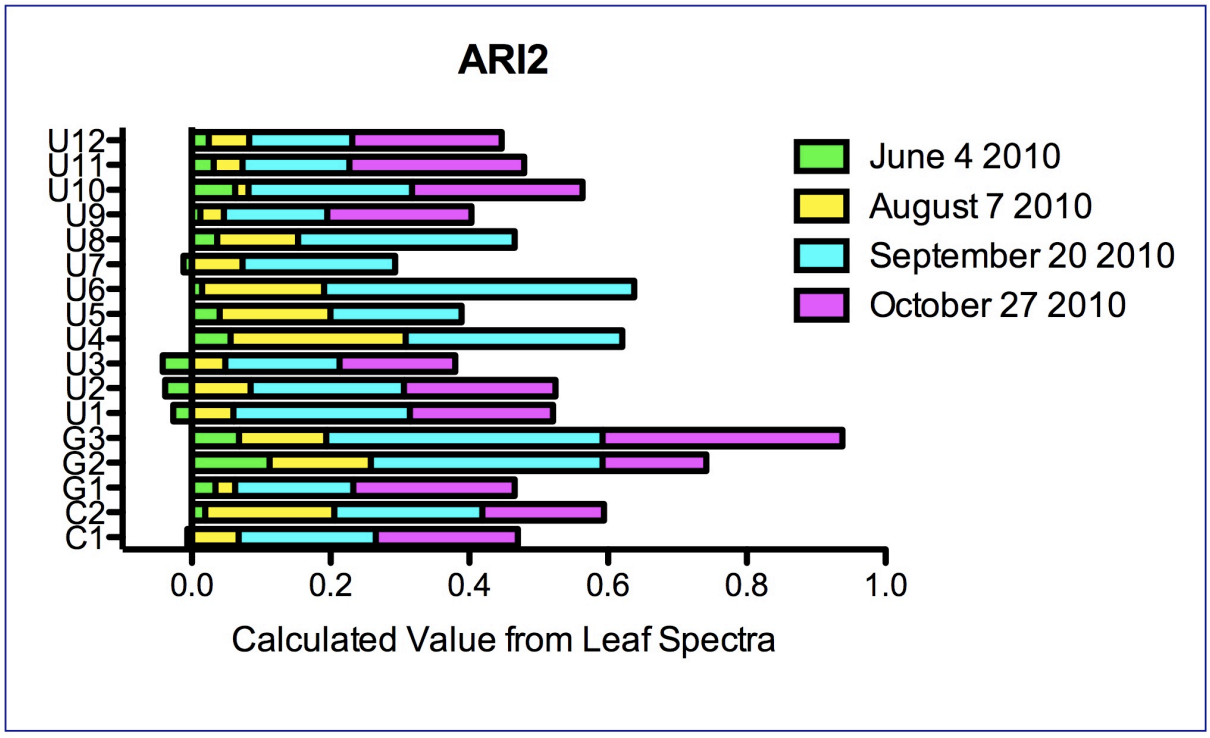

Figure 10 : PSRI and ARI2 results for each collection date

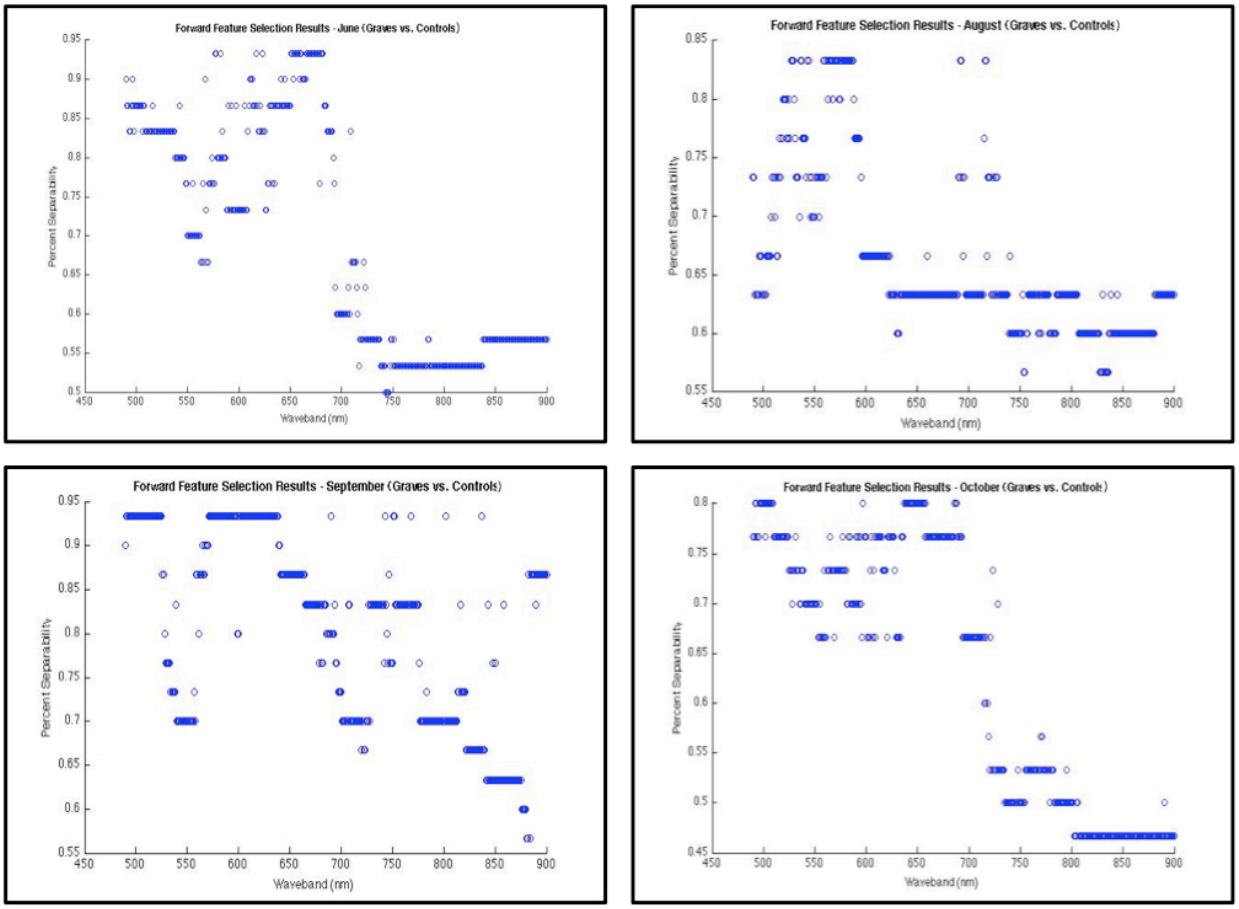

Figure 11 : Forward Feature Selection results for graves vs. Controls for each collection date

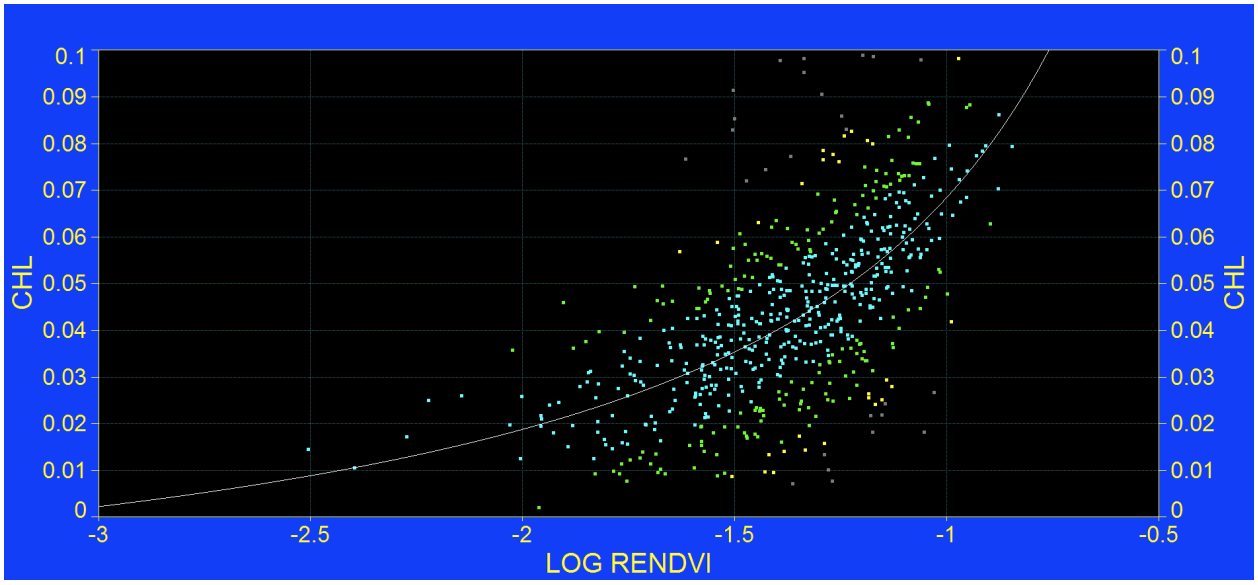

Figure 12 : Computed prediction curve for vegetation chlorophyll content

Figure 13 : Potential grave areas from CASI imagery computed using the Chl prediction curve

Table 1 : Dummy variable analysis over ground chlorophyll data

	Chl Content		
	Controls	Graves	P>|t|
June 4 2010	0.0312	0.0459	0
August 7 2010	0.0472	0.0078	0.205
September 20 2010	0.0387	0.0161	0
October 27 2010	0.0223	0.0099	0.014

Table 2 : Overall classification errors for the normal densities linear classifier

	Normal Densities Linear				
	June	**August**	**September**	**October**	**All Months**
C1,C2	0.15	0.28	0.22	0.35	0.25
U1	0.09	0.25	0.25	0.11	0.15
U2	0.25	0.13	0.13	0.19	0.19
U3	0.09	0.13	0.22	0.16	0.21
U4	0.03	0.03	0.06	N/A	0.16
U5	0.13	0.13	0.03	N/A	0.17
U6	0.13	0.28	0.22	N/A	0.18
U7	0.22	0.25	0.06	N/A	0.15
U8	0.16	0.16	0.25	N/A	0.18
U9	0.16	0.13	0.22	0.13	0.18
U10	0.16	0.16	0.31	0.19	0.24
U11	0.25	0.19	0.31	0.09	0.24
U12	0.16	0.22	0.16	0.22	0.24

Table 3 : Overall classification errors for the NN by backpropagation rule classifier

	NN by Backpropagation rule				
	June	**August**	**September**	**October**	**All Months**
C1,C2	0.19	0.50	0.18	0.29	0.40
U1	0.09	0.11	0.13	0.15	0.23
U2	0.00	0.24	0.13	0.25	0.22
U3	0.09	0.28	0.26	0.13	0.25
U4	0.13	0.03	0.11	N/A	0.23
U5	0.13	0.10	0.06	N/A	0.22
U6	0.09	0.16	0.03	N/A	0.18
U7	0.26	0.09	0.24	N/A	0.18
U8	0.00	0.15	0.22	N/A	0.22
U9	0.21	0.25	0.25	0.16	0.22
U10	0.25	0.19	0.13	0.18	0.27
U11	0.24	0.19	0.24	0.19	0.24
U12	0.28	0.28	0.14	0.25	0.25

Table 4 : Overall classification errors for the Parzen classifier

	Parzen				
	June	**August**	**September**	**October**	**All Months**
C1,C2	0.25	0.39	0.20	0.20	0.38
U1	0.19	0.11	0.08	0.13	0.20
U2	0.08	0.26	0.20	0.22	0.22
U3	0.24	0.26	0.24	0.28	0.23
U4	0.22	0.03	0.20	N/A	0.20
U5	0.26	0.13	0.03	N/A	0.20
U6	0.24	0.15	0.03	N/A	0.20
U7	0.19	0.32	0.19	N/A	0.17
U8	0.20	0.26	0.21	N/A	0.20
U9	0.28	0.28	0.25	0.26	0.24
U10	0.26	0.22	0.19	0.17	0.24
U11	0.15	0.28	0.23	0.26	0.23
U12	0.20	0.19	0.11	0.26	0.25

Table 5 : Overall classification errors for the normal densities quadratic classifier

	Normal Densities Quadratic				
	June	**August**	**September**	**October**	**All Months**
C1,C2	0.41	0.49	0.58	0.58	0.19
U1	0.67	0.41	0.72	0.72	0.13
U2	0.43	0.50	0.72	0.72	0.15
U3	0.70	0.70	0.72	0.68	0.13
U4	0.30	0.70	0.43	N/A	0.75
U5	0.29	0.35	0.72	N/A	0.36
U6	0.68	0.68	0.33	N/A	0.41
U7	0.72	0.69	0.72	N/A	0.63
U8	0.57	0.66	0.72	N/A	0.55
U9	0.63	0.68	0.72	0.72	0.13
U10	0.59	0.64	0.72	0.72	0.13
U11	0.72	0.45	0.48	0.72	0.13
U12	0.72	0.72	0.43	0.72	0.13

Table 6 : Overall classification errors for the NN by Levenberg-Marquardt rule classifier

	NN by Levenberg-Marquardt rule				
	June	**August**	**September**	**October**	**All Months**
C1,C2	0.08	0.28	0.18	0.30	0.18
U1	0.09	0.09	0.16	0.16	0.08
U2	0.03	0.16	0.09	0.22	0.16
U3	0.09	0.13	0.22	0.13	0.20
U4	0.13	0.03	0.09	N/A	0.16
U5	0.09	0.13	0.00	N/A	0.11
U6	0.09	0.19	0.03	N/A	0.14
U7	0.16	0.09	0.03	N/A	0.16
U8	0.00	0.03	0.19	N/A	0.17
U9	0.22	0.22	0.18	0.30	0.21
U10	0.16	0.16	0.13	0.16	0.29
U11	0.19	0.09	0.28	0.22	0.17
U12	0.27	0.25	0.06	0.13	0.20